Journal of Luminescence 190 (2017) 267–271

Contents lists available at ScienceDirect

Journal of Luminescence

journal homepage: www.elsevier.com/locate/jlumin

Peculiarities of intrinsic luminescence excited by pulsed electron beam in CsI and CsI:CO_3

V. Yakovlev[a], L. Trefilova[b,*], A. Lebedynskiy[c], A. Karnaukhova[a], V. Alekseev[c]

[a] Tomsk Polytechnic University, 30 Lenin Avenue, Tomsk 634034, Russian Federation
[b] National University of Civil Protection, 94 Chernyshevska Street, Kharkov 61023, Ukraine
[c] Institute for Scintillation Materials, NAS of Ukraine, 60 Nauky Avenue, Kharkov 61001, Ukraine

A B S T R A C T

The spectra and decay kinetics of STE luminescence arising under a pulsed electron beam (E_{ex} = 0.25 MeV, $t_{1/2}$ = 15 ns, W = 3 mJ/cm^2) in CsI and CsI:8.3·10^{-3}CO_3 mol% within a temperature range of 80 K ÷ 450 K, are examined. It is found that carbonate ions cause a drastic shortening of the intrinsic luminescence decay time at room temperature. The observed distinction in the UV-luminescence decay kinetics of CsI and CsI:CO_3 is due to different temperature behavior of the decay time τ_{slow} in the slow stage of the exponential decay kinetics at temperatures above 200 K. The presented results are interpreted in terms of the existence of "off-center" excitons with different structure morphology in CsI lattice.

1. Introduction

Undoped (or "pure") CsI crystal applied as a fast scintillator responds to irradiation by fast-decaying luminescence, whose spectrum at room temperature consists of one band peaking at 4.1 eV. The origin of this fast-decaying intrinsic luminescence has not yet been completely understood. It was found [1] that the addition of Mg^{2+} ions in the melt leads to shortening of the scintillation pulse duration of the CsI crystal. According to the authors [1], Mg^{2+} ions act as a good scavenger to get rid of O^{2-} ions responsible for the slow decay component of "pure" CsI scintillation pulse. We examined CsI doped with various oxygen-containing anions and found 4.1 eV luminescence decay kinetics to be affected only by carbonate ions shortening drastically the duration of the scintillation pulse [2]. This experimental result can provide the clue to the origin of the intrinsic luminescence making CsI quickly responsive to irradiation at room temperature. The aim of this paper was to clarify the nature of the processes responsible for the intrinsic luminescence decay kinetics of pure CsI and CsI:CO_3 crystals.

2. Experimental procedures

CsI and CsI:CO_3 ingots were grown from the special purity grade salt CsI by the Stockbarger technique in evacuated quartz ampoules. The presence of CO_3^{2-} ions was monitored by the vibration absorption spectra measured by UR-20 spectrophotometers. Any bands were not found in IR absorption spectra of CsI, and only the bands typical of CO_3^{2-} ions were revealed in the spectrum of CsI:CO_3. The concentration of CO_3^{2-} ions was evaluated in mol% by the absorption coefficient in the deformation band peaking at 878 cm^{-1} as it was described in [3]. The studied samples of CsI and CsI:CO_3 containing 8.3·10^{-3} mol% of CO_3^{2-} ions were cut out in the shape of a rectangular plate with the dimensions 10 × 10 × 2 mm^3.

The cathodoluminescence was excited with an electron pulse (the average electron energy E_{ex} = 0.25 MeV, the pulse duration $t_{1/2}$ = 15 ns and the power density W = 3 mJ/cm^2) generated by a GIN-600 electron accelerator and registered by an optical spectrometer consisting of an MDR-3 monochromator, a FEU-106 photomultiplier and a LeCroy digital oscilloscope. The cathodoluminescence oscillograms were registered for photons with a certain energy within a range of 2.0–5.0 eV at a fixed temperature within a temperature range of 80–450 K. Then the oscillograms were converted into the luminescence kinetics curves in order to determine the parameters of the luminescence pulse, as well as to plot the luminescence spectrum at any time delay with 7 ns resolution. The cathodoluminescence spectra were corrected for the dispersion of the monochromator and the spectral sensitivity of the photomultiplier.

3. Experimental results

Fig. 1 shows the normalized spectra of intrinsic UV-luminescence measured immediately after irradiation of CsI and CsI:CO_3 crystals with an electron pulse at 295 K. Both spectra are characterized by the same

* Corresponding author.
E-mail address: laratrefilova@ukr.net (L. Trefilova).

http://dx.doi.org/10.1016/j.jlumin.2017.05.044
Received 6 March 2017; Accepted 15 May 2017
Available online 16 May 2017

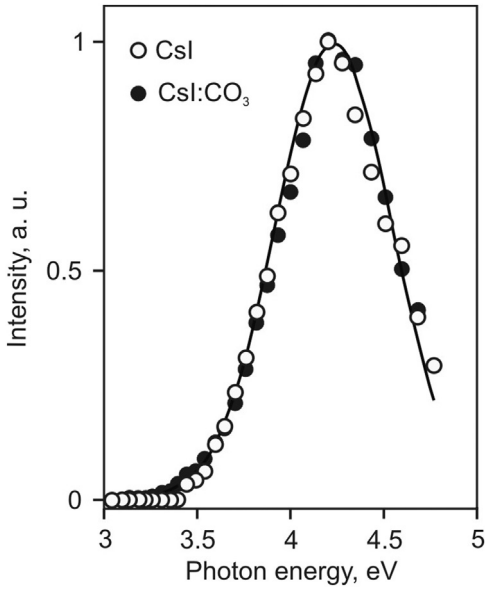

Fig. 1. Cathodoluminescence spectra of CsI and CsI:CO_3 at T = 295 K.

broad band peaking at 4.1 eV. Unlike the spectra, the intrinsic luminescence decay oscillograms of CsI and CsI:CO_3 crystals have different shape (Fig. 2). The sum of two exponents with the decay time τ_{fast} = 15 ns and τ_{slow} = 120 ns fits the 4.1 eV luminescence decay curve of CsI. Our fitting is in good agreement with the data obtained by Nishimura [4] under two-photon excitation of CsI. It should be noted, however, that in comparison with CsI, the slow component with τ_{slow} = 120 ns in the 4.1 eV luminescence decay kinetics of CsI:CO_3 is virtually absent. The mono-exponential decay of the luminescence in CsI:CO_3 crystal testifies that CO_3^{-2} ions drastically affect the kinetics parameters of the intrinsic luminescence of CsI. This experimental result is non-trivial, because the 4.1 eV luminescence is considered to be caused by the radiative annihilation of self-trapped excitons (STE's) in perfect lattice places [4–7]. It seems important therefore to establish the origin of the luminescence centers responsible for the fast and slow compo-

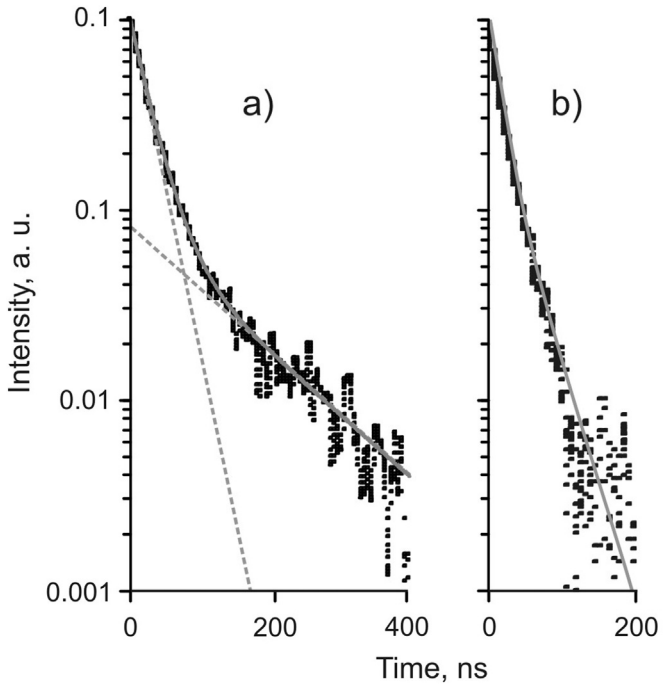

Fig. 2. Cathodoluminescence pulse decay curves at 4.1 eV for CsI (a) and CsI:CO_3 (b) at 295 K.

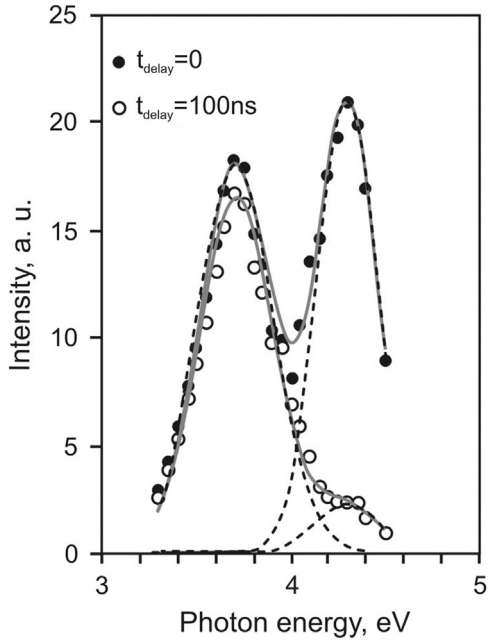

Fig. 3. Luminescence spectra registered with different time delay after the electron pulse depletion of CsI at T = 80 K. Full and empty circles - experimental values; dashed lines - fitting Gaussians; solid lines - the sum of the Gaussians.

nents of the 4.1 eV luminescence decay kinetics of CsI.

To reveal regularities of the processes governing by the decay kinetics, the temperature behavior of the intrinsic luminescence in both crystals was examined within a temperature range of 80–450 K. As one can see in Fig. 3, the luminescence spectrum of pure CsI at 80 K contains two bands peaking at 4.3 and 3.7 eV According to [4–7], both bands are caused by radiative annihilation of STE's with $(I_2^-e^-)^*$ structure. The low energy band at 3.7 eV is due to the radiative transition of STE from the triplet state. At 4.3 eV the high energy band that becomes σ-polarized at T > 11 K, is considered to be caused by the singlet-singlet transition [6]. The decay kinetics of STE luminescence at 80 K can be described as follows. The 3.7 eV luminescence decays exponentially with the decay time equal to 1.0 μs (Fig. 4, curve 1). The sum of the two exponents fits the decay kinetics of the luminescence at 4.3 eV (Fig. 4, curve 2). The fast decay component of the 4.3 eV

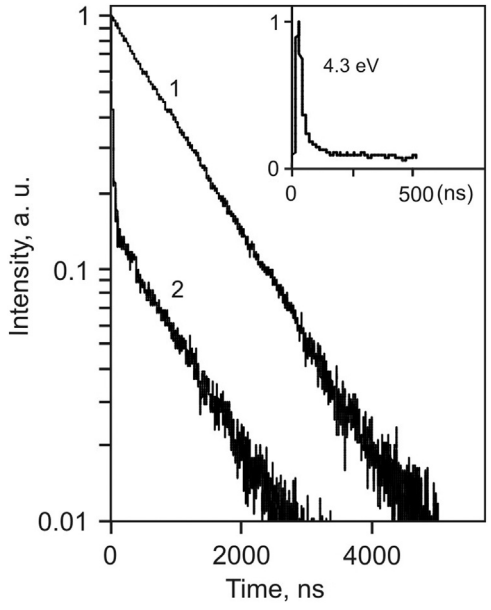

Fig. 4. Oscillograms of luminescence pulse at 3.7 eV (1) and 4.3 eV (2) for CsI at T = 80 K.

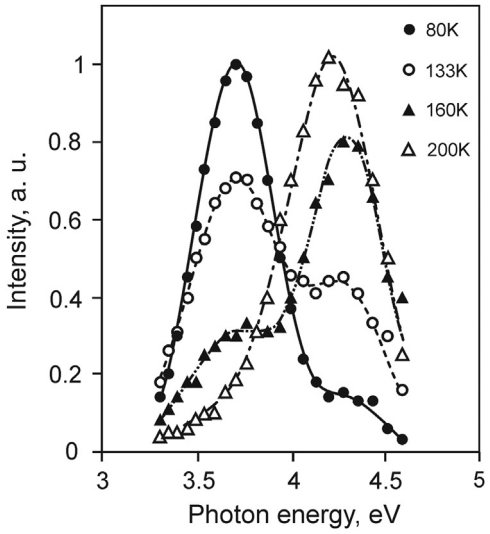

Fig. 5. Spectra of slow-decaying intrinsic luminescence measured for CsI with 100 ns delay at different temperatures.

luminescence is characterized by the decay time equal to $\tau = 10$ ns, whereas the decay time of the slow decay component of the 4.3 eV luminescence matches the decay time of the 3.7 eV luminescence decaying mono-exponentially.

The temperature rise above 80 K causes the increase in intensity for the slow decay component of the 4.3 eV luminescence, which is accompanied by the decrease in intensity of the 3.7 eV luminescence. Fig. 5 presents the spectra measured with the 100 ns time delay at different temperatures.

Decomposition of these spectra into Gaussians shows that the temperature rise above 80 K leads to broadening of both bands, as well as to the red shift of the high energy band (Table 1). Therefore, in fact only one broad band peaking at 4.1 eV is observed in the intrinsic luminescence spectrum at room temperature (Fig. 1).

The temperature dependences of the 3.7 and 4.3 eV luminescence intensity measured for CsI with the 100 ns time delay after the electron pulse depletion is shown in Fig. 6. It should be noted that in general the temperature behavior of the spectral-kinetic parameters of UV-luminescence excited by the pulsed electron beam is the same as the one observed by Nishimura [4] under two-photon excitation of CsI at temperatures above 80 K. All the above results prove that the transition of STE from the triplet state to the excited singlet state is assisted by phonons.

The temperature rise from 80 K changes not only the spectral composition, but also the decay kinetic of the intrinsic luminescence. Being mono-exponential at 80 K, the slow stage of the decay kinetics assumes one more (faster) component, so that the double-exponential function fits the slow decay component at a temperature above 110 K:

$$I(t) = I_{slow}\cdot\exp(-t/\tau_{slow}) + I_{fast}\cdot\exp(-t/\tau_{fast}), \quad (1)$$

where I_{slow}, I_{fast} is the intensity of the slow and fast component at $t=0$, respectively; τ_{slow}, τ_{fast} are the decay times.

The examples of the double exponential functions fitting for the experimental decay curves are presented in Fig. 7. It should be noted

Table 1
Parameters of elementary bands in the intrinsic luminescence spectra of CsI.

T, K	E_{m1}, eV	FWHM, eV	E_{m2}, eV	FWHM, eV
78	4.3	0.41	3.7	0.47
133	4.3	0.47	3.7	0.57
200	4.22	0.53	3.7	0.64
295	4.15	0.58	3.7	0.71

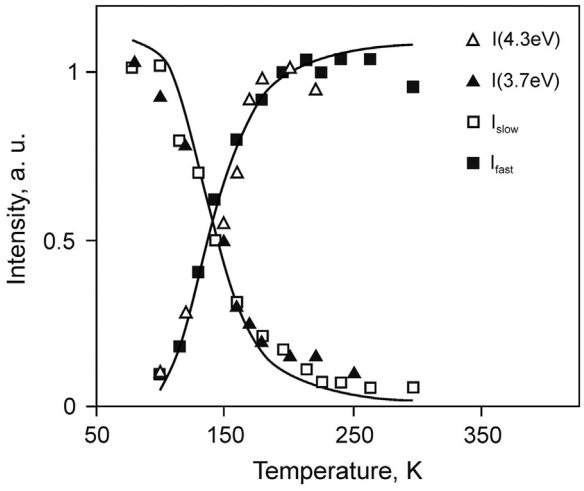

Fig. 6. Intensities of luminescence bands peaking at 4.3 eV and 3.7 eV vs. temperature; intensities of the fast I_{fast} and slow I_{slow} luminescence decay components vs. temperature. The best fitting by Eqs. (11) and (12) is shown by solid lines.

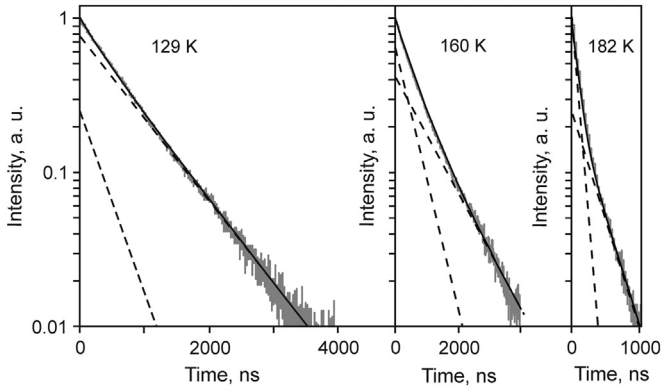

Fig. 7. UV-luminescence pulse decay curves for CsI at different temperatures. Broken lines - the experimental curves; solid lines - the fitting curves by the double exponential Eq. (1); dashed lines - the exponential components of the fitting curves.

that luminescence whose intensity falls down with the temperature has identical spectra in both the slow and fast decay stages. As one can see in Fig. 6, the temperature dependences of $I_{slow}(T)$ and $I_{fast}(T)$ are inverse; the reduction in the share of the slow component and the increase in the share of the fast component at the temperature rise completely match the decrease of the 3.7 eV luminescence intensity and the increase of the 4.3 eV luminescence intensity, respectively.

The data obtained for CsI:CO_3 are identical to those shown in Figs. 3–7 for CsI. Fig. 8 demonstrates the temperature dependences of the parameters of STE luminescence kinetics for CsI and CsI:CO_3 crystals. As it is seen, the luminescence of both crystals decays at the fast stage with the decay time τ_{fast} which has approximately the same value at a given temperature in the whole temperature range. However, the temperature behavior of decay time in the slow stage is different for these crystals. As the temperature rises from 80 K to 295 K, there is observed a monotonic shortening of τ_{slow} from 1 μs to ~ 30 ns for CsI:CO_3. The behavior of $\tau_{slow}(T)$ dependence for CsI is similar to that for CsI:CO_3 only in the low temperature range, but at higher temperatures τ_{slow} becomes equal to 120 ns and remains unchanged at temperatures from 230 K up to 320 K.

4. Discussion

The above results can be briefly summarized as follows. With the temperature rise above 110 K, the phonon-assisted transitions of STE's from the triplet to the singlet excited state cause the intensity increase

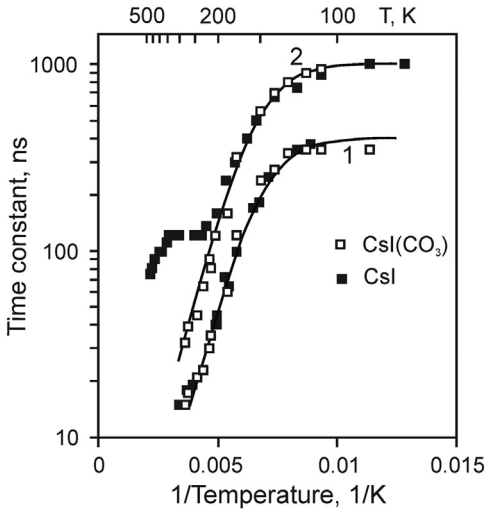

Fig. 8. Decay constants τ_{fast} (1) and τ_{slow} (2) of the intrinsic luminescence vs. reciprocal temperature for CsI and CsI(CO_3). The best fitting by Eqs. (13) and (14) is shown by solid lines.

of σ-polarized luminescence band peaking at 4.3 eV, which is related to the formation of a new type excitons during the irradiation pulse depletion. These excitons differ from those arising at 80 K by the lifetime prior to their spontaneous radiative annihilation (Figs. 6 and 7). As shown above, both types of excitons have the same luminescence spectrum that testifies to identical structure of their electron levels.

According to existing conceptions, STE which consists of two halide hole and a bound electron can be formed in an alkali halide with different spatial separation of the hole and electron component. There are different types of STE's: on-center STE in which a self-trapped hole V_k and a bound electron are centered at the midpoint between two nearest halide sites [8,9]; "weak-off-center" and "strong-off-center" STE characterized by small and large off-center shift of V_k core, respectively [10–14]. "Strong-off-center" STE is regarded to be nearly identical to a close F-H pair. STE's with different type of structure morphology are separated by small energy barriers on their common adiabatic potential energy surface [13,14]. The temperature rise leads to monotonic off-center displacement of V_k core, thereby increasing the degree of separation of the electron and hole STE components to form eventually the pair of the separated in space F and H centers [14–16]. The energy barrier separating the lowest relaxed state of STE from the state corresponding to F, H - defect pair in CsI crystal is equal to 0.22 eV [17]. Fig. 9 demonstrates (in blue line) the section of the common adiabatic potential energy surface for the states of the two types of "off-center" STE's and the F-H defect pair state, which completely corresponds to the observed regularities. The coordinate R characterizes the spatial separation of the electron and hole components of STE's. The energy diagrams of the radiative singlet and triplet states for off-center STE's of both types are shown in the configuration coordinates in the figure by black lines.

The temperature behavior of the intrinsic luminescence kinetics is determined by the existence of the energy barrier ΔE between the triplet and excited singlet levels. This barrier also separates the states of the "weak off-center" and "strong off-center" STE's whose population is denoted by n_1 and n_2, respectively (Fig. 9). This statement is based on the fact that the temperature dependences of $I_{4.3\ eV}(T)$ and $I_{3.7\ eV}(T)$ coincide with those of $I_{fast}(T)$ and $I_{slow}(T)$, respectively (Fig. 6). Since the capture of conduction electrons by self-trapped holes is regarded to be the main channel for STE formation in alkali halides under irradiation, we will assume that the total number of STE arising by the moment of an irradiation pulse depletion ($t_{delay} = 0$) is temperature-independent:

$$N_{t=0} = n_{10} + n_{20} = Const(T). \tag{2}$$

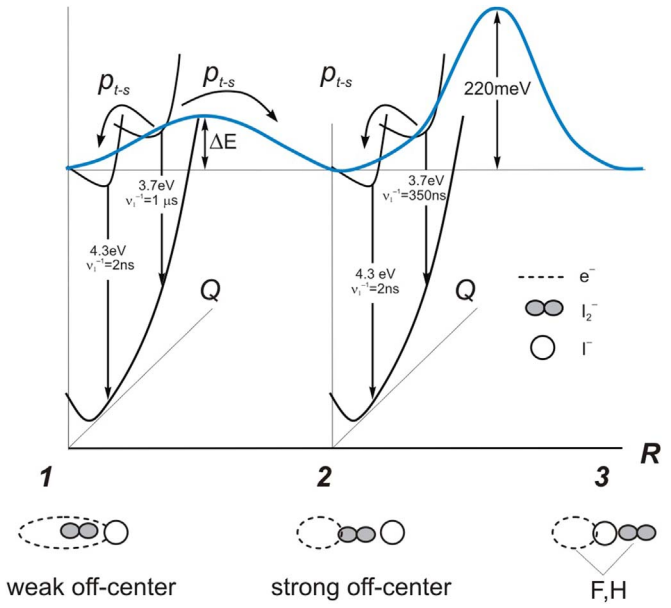

Fig. 9. Section of adiabatic potential surface common for the states of "off-center" STE of the two types and of F-H defect pair state.

During an irradiation pulse (15 ns), the thermodynamic equilibrium is established in the system, and the initial population of the levels is expressed in the form:

$$n_{10}(T) = N_{t=0}(1 + A\cdot\exp(-\Delta E/kT))^{-1}, \tag{3}$$

$$n_{20}(T) = N_{t=0}\cdot[1 - (1 + A\cdot\exp(-\Delta E/kT))^{-1}]. \tag{4}$$

The changes of the level population after the irradiation pulse depletion are realized by intracenter interlevel triplet-singlet transitions, and can be found by solving the differential equations

$$-dn_1 = n_1\cdot(\nu_1 + p_{t-s})\cdot dt, \tag{5}$$

$$-dn_2 = n_2\cdot(\nu_2 + p_{t-s})\cdot dt, \tag{6}$$

where $\nu_i = 1/\tau_i \neq f(T)$ is the frequency of spontaneous radiative electron transitions; $p_{t-s} = \omega_i\cdot\exp(-\Delta E/kT)$ is the probability for phonon-assisted transition of STE from the triplet to the excited singlet state followed by fast ($\tau = 2$ ns [4]) radiative transition to the ground state. Decrease in the population of the levels with time is expressed as

$$n_1(t) = n_{10}\cdot\exp(-(\nu_1 + p_{t-s})\cdot t), \tag{7}$$

$$n_2(t) = n_{20}\cdot\exp(-(\nu_2 + p_{t-s})\cdot t). \tag{8}$$

The luminescence intensity goes down with time as follows:

$$I_1(t) = \nu_1\cdot n_{10}\cdot\exp(-(\nu_1 + p_{t-s})\cdot t) = I_{slow}\cdot\exp(-t/\tau_{slow}), \tag{9}$$

$$I_2(t) = \nu_2\cdot n_{20}\cdot\exp(-(\nu_2 + p_{t-s})\cdot t) = I_{fast}\cdot\exp(-t/\tau_{fast}). \tag{10}$$

In accordance with (3), (4) and (7), (8), the temperature dependences of the initial intensities I_{slow}, I_{fast} and the decay time τ_{slow}, τ_{fast} are defined by the following equations:

$$I_{slow}(T) = \nu_1\cdot n_{10} = \nu_1\cdot N_{t=0}(1 + A\cdot\exp(-\Delta E/kT))^{-1}, \tag{11}$$

$$I_{fast}(T) = \nu_2\cdot n_{20} = \nu_2\cdot N_{t=0}\cdot[1 - (1 + A\cdot\exp(-\Delta E/kT))^{-1}], \tag{12}$$

$$\tau_{slow} = (\nu_1 + \omega_1\cdot\exp(-\Delta E/kT))^{-1}, \tag{13}$$

$$\tau_{fast} = (\nu_2 + \omega_2\cdot\exp(-\Delta E/kT))^{-1}. \tag{14}$$

The curves calculated by Eqs. (11)–(14) (solid lines in Figs. 6 and 8) well fit the experimental data. Table 2 lists the best fit parameter values for the equations.

Table 2
The values of parameters in Eqs. (11)–(14) obtained by the fitting to the data presented in Fig. 6 and Fig. 8.

Parameters	ν, c^{-1}	ω, c^{-1}	A, a. u.	ΔE, meV
τ_{slow}	$1.0 \cdot 10^6$	$1.5 \cdot 10^9$		95
τ_{fast}	$2.5 \cdot 10^6$	$4.5 \cdot 10^9$		95
I_{slow}			2400	95
I_{fast}			2400	95

Thus, the presence of the fast and slow stages in UV-luminescence decay kinetics for CsI in 110 ÷ 200 K temperature range is due to the creation of STE's of two morphologies. It is also noteworthy that at high temperatures the experimental dependence $\tau_{slow}(T)$ for CsI has a pronounced "shoulder" which is not observed in the said dependence for CsI:CO_3. In our opinion, the "shoulder" is a manifestation of further structural transformations of STE resulting in the formation of "off-center" STE's with the third type of structure morphology that directly precedes the formation of the Frenkel defect pairs in CsI. Analysis of the temperature dependences shows that τ_{slow} of CsI decreases at the temperature rise above 320 K according to the Mott's law with an activation energy of 0.22 eV, that corresponds to the activation energy for the rise of F-center yield [17]. The coincidence of the activation energies for two inverse processes indirectly confirms the above assumption. In such a case, the absence of the "shoulder" on the dependence $\tau_{slow}(T)$ for CsI(CO_3) may signify that the carbonate ions CO_3^{2-} make the formation of the third type "off-center" STE impossible. Unlike other oxygen-containing anions, CO_3^{2-} ion substitutes I^- ion in CsI lattice, and its excess negative charge is compensated by the positively charged anion vacancy which gives rise to the formation of an impurity-vacancy dipole [CO_3^{2-}-v_a^+] [18,19]. The third type "off-center" STE's with spatially separated electron and hole components are also electric dipoles, therefore, one of possible causes of their suppression may be the Coulomb interaction between "off-center" STE's and the impurity-vacancy dipoles [CO_3^{2-}- v_a^+].

5. Conclusion

The data obtained for CsI and CsI:CO_3 crystals by means of time-resolved cathodoluminescent spectroscopy made it possible to reveal two structure morphologies of "off-center" STE's, which are characterized by identical structure of electron levels, but different lifetime prior to their spontaneous radiative annihilation. All the three phonon-assisted processes leading to (i) the yield rise of the fast decay component of STE luminescence, (ii) the intensity increase of the luminescence band peaking at 4.3 eV band and (iii) shortening of the STE lifetime with temperature rise, were found to be governed by the energy barrier Δ E separating the triplet and excited singlet levels of STE. Regarding the influence of carbonate impurity, the observed shortening of the intrinsic luminescence decay time at temperatures above 200 K may be caused by suppression of the channel of the third type "off-center" STE formation due to the presence of impurity-vacancy dipoles [CO_3^{2-}-v_a^+] in the lattice.

References

[1] V.L. Cherginets, T.P. Rebrova, Yu.N. Datsko, V.F. Goncharenko, N.N. Kosinov, V.Yu Pedash, Mater. Lett. 65 (2011) 2416–2418.
[2] L. Trefilova, V. Yakovlev, N. Ovcharenko, A. Grippa, A. Mitichkin, Book of abstracts of 4th International Congress on Energy Fluxes and Radiation Effects, Tomsk, Russia, 2014, p. 431.
[3] L. Trefilova, B. Grinyov, V. Alekseev, A. Mitichkin, V.Yu Yakovlev, A. Meleshko, IEEE Trans. Nucl. Sci. 55 (2008) 1263–1269.
[4] H. Nishimura, M. Sakata, T. Tsujimoto, M. Nakayama, Phys. Rev. B. 51 (1995) 2167–2172.
[5] T. Iida, Y. Nakaoka, J.P. von der Weid, M.A. Aegerter, J. Phys. C 13 (1980) 983–992.
[6] J.P. Pellaux, T. Iida, J.P. von der Weid, M.A. Aegerter, J. Phys. C 13 (1980) 1009–1018.
[7] H. Lamatsch, J. Rossel, E. Saurer, Phys. Status Solidi B 48 (1971) 311–318.
[8] M.N. Kabler, Phys. Rev. 136 (1964) A1296–A1302.
[9] T. Matsumoto, T. Kavata, A. Miyamoto, K. Kan'no, J. Phys. Soc. Jpn. 61 (1992) 4229–4241.
[10] D. Block, A. Wasiela, Y. Meric D`Aubigne, J. Phys. C: Solid State Phys. 11 (1978) 4201–4211.
[11] C.H. Leung, G. Brunet, K.S. Song, J. Phys. C: Solid State Phys. 18 (1985) 4459–4470.
[12] G. Brunet, C.H. Leung, K.S. Song, Solid State Commun. 53 (1985) 607–609.
[13] R.T. Williams, Hanli Liu, G.P. Williams, Kevin J. Platt, Phys. Rev. Lett. 66 (1991) 2140–2143.
[14] N. Itoh, T. Eshita, R.T. Williams, Phys. Rev. B: Condens. Matter 34 (1986) 4230–4234.
[15] R.T. Williams, K.S. Song, W.L. Faust, C.H. Leung, Phys. Rev. B 33 (1986) 7232.
[16] K.S. Song, R.C. Baetzold, Phys. Rev. B 46 (1992) 1960–1969.
[17] E.S. Gafiatulina, S.A. Chernov, V.Y. Yakovlev, Phys. Solid State 40 (1998) 586–590.
[18] E.L. Vinograd, V.I. Goriletsky, S.P. Korsunova, A.M. Kudin, A.I. Mitichkin, A.N. Panova, A.V. Radkevich, K.V. Shakhova, L.N. Shpilinskaja, Opt. Spectrosc. 75 (1993) 966–1000.
[19] V. Yakovlev, L. Trefilova, A. Lebedinsky, Z. Daulet, I. Dubtsov, J. Lumin. 173 (2016) 34–37.